Splicing inactivation generates hybrid mRNA-snoRNA transcripts targeted by cytoplasmic RNA decay

Yanru Liu[1,2], Samuel DeMario[1], Kevin He[1], Michelle Gibbs[1], Keaton Barr[1] and Guillaume F. Chanfreau[1,3]

1. Department of Chemistry and Biochemistry, UCLA, Los Angeles, CA 90095, United States of America

2. Present address: Department of Molecular Biology and Genetics, Cornell University, Ithaca, NY 14853-2703

3. Molecular Biology Institute, UCLA, Los Angeles, CA 90095, United States of America

*Corresponding Author

Email: guillom@chem.ucla.edu

Abstract

Many small nucleolar RNAs are processed from introns of host genes, but the importance of splicing for proper biogenesis and the fate of the snoRNAs is not well understood. Here we show that inactivation of splicing factors or mutation of splicing signals leads to the accumulation of incorrectly processed hybrid mRNA-snoRNA transcripts (hmsnoRNA). HmsnoRNAs are processed to the mature 3′-end of the snoRNA by the nuclear exosome and bound by snoRNP proteins, but they are targeted by the major cytoplasmic mRNA decay pathway due to their mRNA-like 5′-extensions. These results show that completion of splicing is required for full and accurate processing of intron-encoded snoRNAs and that splicing defects lead to degradation of hybrid mRNA-snoRNA species by cytoplasmic decay, uncovering a novel aspect of the importance of splicing for the biogenesis of intron encoded snoRNAs.

Introduction

Small nucleolar RNAs (snoRNAs) are non-coding RNAs that guide snoRNP-mediated 2′-O-methylation or pseudouridylation of pre-ribosomal RNAs precursors and other stable RNAs [1,2,3]. These snoRNAs are classified in two major families: the C/D and H/ACA classes, which guide 2′-O-methylation and pseudouridylation of their substrates, respectively. The importance of correct snoRNA expression is underscored by the fact that defects in snoRNA metabolism are linked to multiple pathologic processes including cancer [4,5], Prader-Willi syndrome [6], and metabolic stress [7]. SnoRNAs are found in many different genomic contexts [2,8]. In mammalian genomes, many snoRNAs are present in the introns of host genes, but they can also be generated from lncRNAs. Alternative splicing of pre-mRNAs containing multiple snoRNAs can influence the levels of snoRNAs expressed from these host genes [9]. The site of transcription initiation of the host gene, or the genomic context can also modulate the levels of expression and tissue specificity of snoRNAs[10]. In plants, snoRNAs are often generated from polycistronic transcription units[8]. In the budding yeast *S.cerevisiae* which has been used extensively to study the mechanisms of snoRNA biogenesis and processing, snoRNA are expressed either from independently transcribed genes, polycistronic snoRNA precursors, or from introns 2,[8]. The synthesis of mature snoRNAs from intronic sequences is thought to occur primarily through splicing of the host gene pre-mRNA. *In vitro* and *in vivo* studies have shown that splicing results in accurate processing of intron-encoded snoRNA in mammalian cells [11]. The current model is that intron-encoded snoRNAs are generated by exonucleolytic trimming of the excised linear introns after completion of the splicing reaction and debranching of the lariat introns. In support of this model, inactivation of the *S.cerevisiae* debranching enzyme Dbr1p results in the accumulation of lariat intron species containing the snoRNAs [12], showing that debranching of the excised intron is critical for processing. However, the production of mature snoRNA can still occur inefficiently in the absence of the debranching enzyme[12], because random hydrolytic cleavage of the lariat intron exposes the cleaved intron to processing by exonucleases or by cleavage by the RNase III enzyme Rnt1p[13]. In addition, some studies have reported splicing-independent processing of intron-encoded snoRNAs [14], either by endonucleolytic cleavage of the

precursors [13,15], or by exonucleolytic processing [16]. In *S.cerevisiae*, the RNase P endonuclease has also been proposed to initiate a processing pathway independent from splicing, by cleaving unspliced pre-mRNAs that host box C/D snoRNAs [17].

Despite the known importance of splicing for the processing of intron-encoded snoRNAs, it is unclear how defects in the spliceosome machinery may impact the fate of intron-encoded snoRNAs. This is an important question, as recent work has shown that defects in 5′-end processing of independently transcribed snoRNAs can result in mislocalization of the unprocessed snoRNAs in budding yeast[18]. Strikingly, very little is known about the impact of spliceosome defects on snoRNA expression. Haploinsufficiency of the core snRNP protein SmD3 results in a reduction in the levels of intron-encoded snoRNAs[19], but the specific molecular effects of this mutation on the biogenesis pathway of intron-encoded snoRNAs have not been investigated. In this study, we have analyzed the impact of inactivating splicing using *trans* and *cis*-acting splicing mutants on the production of intron-encoded snoRNAs in the yeast *S.cerevisiae*. We show that inactivating splicing factors involved in different steps of the spliceosome cycle, or mutating the splicing signal of a host gene result in the accumulation of aberrant, hybrid mRNA-snoRNAs species which share some of the hallmarks of mature snoRNAs, but are degraded by the cytoplasmic mRNA decay pathway. These results highlight the importance of splicing for determining the fate of intron-encoded snoRNAs and show that incorrectly processed intron-encoded snoRNAs are degraded by the general mRNA decay pathway. Our results may also provide some insights onto possible additional effects of genetic diseases that are due to splicing factor mutations.

Results

Inactivation of splicing factors at different stage of the spliceosome cycle results in the accumulation of hybrid mRNA-snoRNA forms of *NOG2/snR191*.

To investigate the importance of the splicing reaction for the processing of intron-encoded snoRNAs, we used the anchor away (AA) technique[20], during which addition of

rapamycin promotes the rapid export of endogenously FRB (*FKBP12*-rapamycin binding domain)-tagged splicing factors to the cytoplasm[20]. The genetic background used for these experiments alleviates the toxic effects of rapamycin and its natural downstream effects on gene regulation [20]. The AA technique results in the nuclear depletion of these factors and in the inactivation of their nuclear functions *in vivo*. To analyze the contribution of splicing factors involved at different steps of the spliceosome cycle, we used strains expressing FRB-tagged versions of Prp5p, Prp28p, Prp16p, Prp18p, Slu7p, and Prp22p. These proteins are involved in various steps of the splicing pathway[21], from spliceosome assembly (Prp5p, Prp28p) to the second catalytic step (Prp16p, Prp18p, Slu7p, Prp22p) and spliceosome recycling (Prp22p). We first analyzed expression of the *NOG2* gene which contains the H/ACA snoRNA snR191 in its intron [22] by Northern blot (Figure 1A). After nuclear depletion of each of these splicing factors, a probe hybridizing to the exon1 of *NOG2* detected the unspliced precursors, but also some RNAs migrating faster than the spliced mRNAs. These RNAs were detected in all the anchor away strains treated with rapamycin, but not prior to rapamycin treatment (band labeled hms on Figure 1B). We first hypothesized that these species might correspond to cleaved 5′-exons that would accumulate due to a second catalytic step defect; however, based on their estimated size (~1100nt), these species are too large to correspond to free 5′ exons. In addition, these species were detected when anchoring away proteins involved prior to the first catalytic step (eg. Prp5p, Prp28p). Furthermore, species migrating faster than the hms RNAs and whose size matches those of cleaved 5′exons (~850nt) were observed only in strains in which second step splicing factors are anchored away (Slu7p, Prp16p, Prp18p, Prp22p), but not in strains in which splicing factors involved prior to the first step are depleted from the nucleus (Prp5p; Prp28p). The fastest migrating species correspond to cleaved 5′-exons that fail to undergo splicing because of second step defects and are labeled E1 in all figures.

Figure 1. Hybrid forms of the *NOG2* mRNA-snR191 snoRNA are produced upon splicing inactivation.

A. Schematic structure of the *NOG2* gene encoding the *snR191* H/ACA snoRNA in its intron, and proposed structure of the *NOG2-snR191* hmsnoRNA. Exons are represented by black boxes and the mature snoRNA by a gray box. Intronic sequences are shown as gray lines. Numbers indicate the length in nucleotides of the different exonic and intronic regions and of the snoRNA. UTR lengths are not included. Black lines with numbers 1-3 indicate the approximate locations of the different riboprobes used for this figure. Boxes and line lengths are not to scale.

B. Northern blot analysis of *NOG2/snR191* in strains expressing anchor-away (AA) FRB-tagged versions of the Slu7p, Prp16p, Prp18p, Prp5p, Prp28p and Prp22p splicing factors. Each FRB tagged strain was grown in normal medium, and then spun down and resuspended in either fresh normal media or shifted to media containing rapamycin for 1hr to promote export of the tagged splicing factor out of the nucleus. Probe#1 was used for the top panel. GAPDH was used as a loading control. US = unspliced pre-mRNA; S = Spliced mRNA; Ab = Aberrant snoRNA.

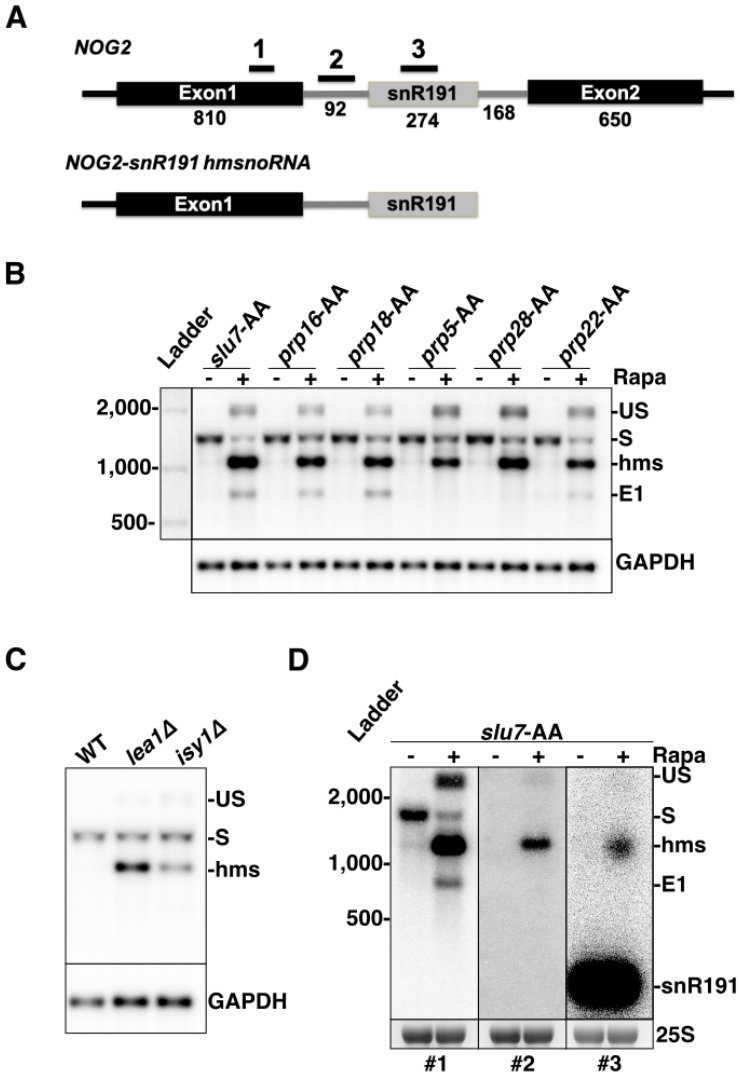

C. WT Northern blot analysis of NOG2 in strains in WT and *lea1*Δ or *isy1*Δ deletion strains. Legend as in (B).

D. Mapping of the hmsnoRNA forms of snR191 using different riboprobes. Shown are northern blots of NOG2/snR191 using riboprobes 1,2 and 3 shown in (A) of RNAs extracted from the Slu7-AA strain before or after 1hr treatment with rapamycin. An ethidium bromide staining of the 25S rRNA is shown as a loading control.

RNAs similar in size to the species labeled hms described above also accumulated in mutants carrying deletions of the non-essential genes encoding the U2 snRNP component Lea1p[23] or the splicing fidelity factor Isy1p[24] (Figure 1C). Therefore, the production of the hms RNAs is due to general defects in spliceosome function rather than to some indirect effects of anchoring away essential splicing factors. Further mapping of the hms RNAs using probes hybridizing to the different regions of *NOG2-snR191* gene (Figure 1A) showed that these species also hybridize to probes complementary to the mature *snR191* snoRNA and to the intronic region preceding the snoRNA (Figure 1D). Based on their approximate size (~1100 nucleotides) and their hybridization patterns, we hypothesized that these RNAs correspond to hybrid mRNA-snoRNA (hmsnoRNA) species containing the mRNA 5′-exon, the intronic segment upstream of the snoRNA, and the entire snoRNA sequence (schematic representation in Figure 1A). The combination of estimated sizes and probe hybridization patterns was consistent with a 3′-end close to that of the mature snoRNA 3′-ends. To test this idea, we mapped the 3′-end of the *NOG2-snR191* hmsnoRNA using a modified 3′-RACE protocol after i*n vitro* polyadenylation of total RNAs. Sequencing of the 3′-RACE products showed that the *snR191* hmsnoRNA 3′-ends match precisely those of mature snoRNAs (Supplemental Figure 1).

HmsnoRNAs can be detected for several intron-encoded C/D box snoRNAs

To extend the results described above for other snoRNAs, we analyzed RNAs accumulating in the Slu7p-AA strain prior to or after rapamycin treatment for several genes expressing box C/D snoRNAs from their introns: *IMD4*/*snR54* (Figure 2A), *TEF4*/*snR38* (Figure 2B) and *ASC1*/snR24 (Figures 2C and 2D). For *IMD4*/*snR54* and *TEF4*/*snR38*, we detected the accumulation of hmsnoRNA species hybridizing to both exon1 and snoRNA probes (Figures 2A and 2B). We performed more detailed mapping of the *ASC1/snR24* hmsnoRNA using four probes hybridizing to different regions of *ASC1* (Figure 2C). The *ASC1-snR24* hmsnoRNA species were detected by the 5′-exon and snoRNA probes (probes 1 and 3), and by an intronic probe located 5′ to the snoRNA (probe 2), but not to a probe hybridizing to the 3′-exon (probe 4; Figure 2D).

Figure 2. HmsnoRNAs can be detected for several intron-encoded box C/D snoRNAs.

A. Northern blot analysis of IMD4/snR54 in RNAs extracted from the Slu7p-AA strain before or after treatment with rapamycin for one hour. Shown are northern blots using probes hybridizing to the 5′-exon or to the mature snoRNA. Labeling of the different species as in Figure 1. *scR1* was used as a loading control.

B. Northern blot analysis of TEF4/snR38 in the Slu7p-AA strain Legends as in (A). LI = Lariat Intron-Exon2 intermediate.

C. Structure of the ASC1/snR24 gene and location of the probes used for differential northern blot analysis in Figure 2D. Legends as in Figure 1A. Boxes and line lengths are not to scale.

D. Northern blot analysis of ASC1/snR24 in the Slu7p-AA strain using probes hybridizing to the indicated regions of the ASC1/snR24 gene. An ethidium bromide staining of the 25S rRNA is shown as a loading control.

E. Analysis of the polyadenylation status of ASC1/snR24. Shown is a northern blot of ASC1/snR24 using a 5′exon probe (#1 in Figure 2C) of RNAs extracted from the Slu7p-FRB tagged strain grown after treatment with rapamycin. T = total RNAs; pA+= polyadenylated RNAs selected by oligodT affinity; pA- = Non-polyadenylated RNAs extracted from the supernatant of the oligodT affinity purification.

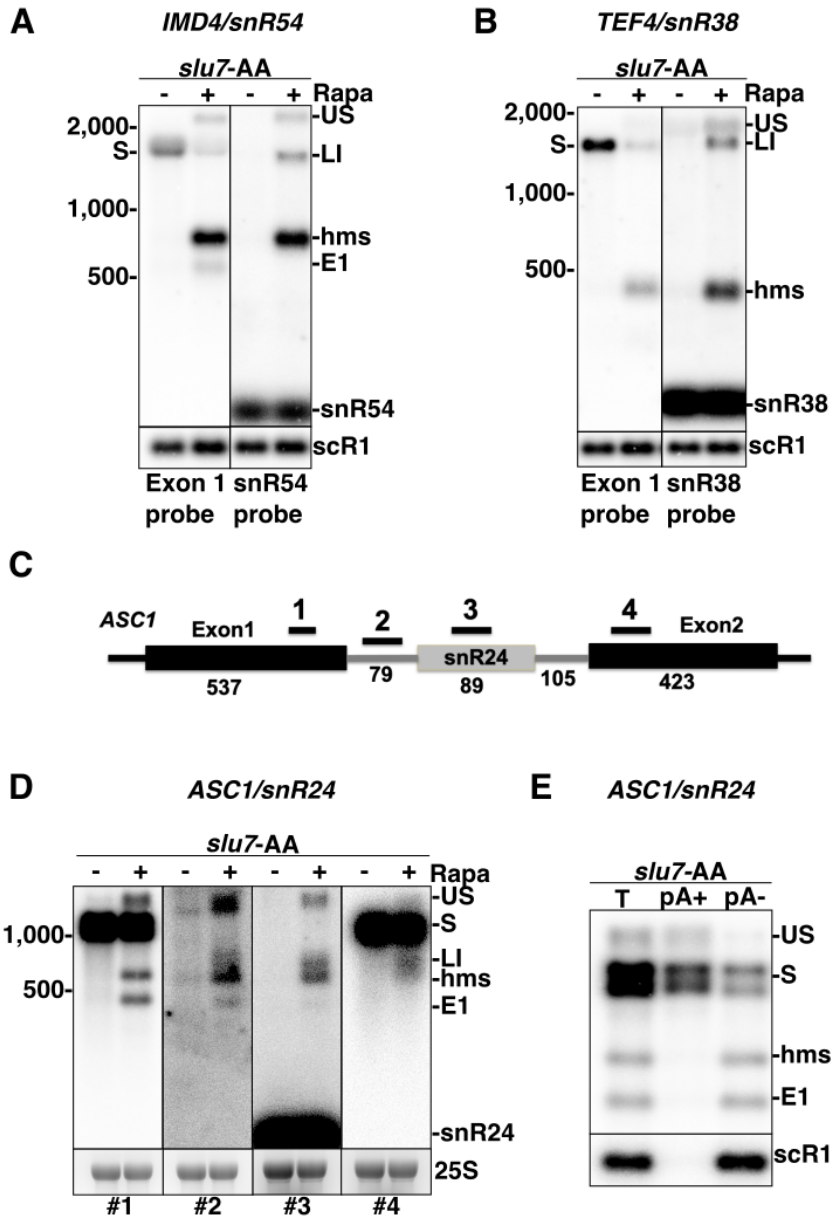

As expected, probe 1 also detected the cleaved 5′-exon intermediate, and probes 2-4 detected the lariat intermediate in the Slu7p-AA strain treated with rapamycin. The estimated size and hybridization patterns of the *ASC1-snR24* hmsnoRNA show that these species correspond to the exon1 of *ASC1*, the first part of the intron and the entire snoRNA sequence that ends close to the mature 3′-end. The estimated size and hybridization patterns of the *IMD4/snR54* and *TEF4/snR38* hmsnoRNAs (Figures 2A and 2B) suggest a similar architecture. In addition, we mapped the 3′-end of the *IMD4/snR54* hmsnoRNA using the modified 3′-RACE previously used for snR191, and found that the *IMD4/snR54* hmsnoRNA was identical to that of the mature *snR54* (Supplemental Figure 1). Thus, splicing inactivation results in the general accumulation of hybrid mRNA-snoRNA species for all intron-encoded snoRNA described here, which belong to both H/ACA and C/D families.

HmsnoRNAs are not polyadenylated but acquire their 3′-ends by exonucleolytic trimming by the exosome.

One possibility that would explain the production of hmsnoRNAs upon splicing inactivation is that in the absence of splicing, premature cleavage and polyadenylation of the unspliced precursors would occur within intronic sequences shortly after the snoRNA, which would generate a hybrid mRNA-snoRNA transcript polyadenylated after the snoRNA mature 3'-end. However, the snR191 and snR54 hmsnoRNA 3′-ends are similar to those of the corresponding mature snoRNAs (Supplemental Figure 1). In addition, northern blot analysis of total and polyadenylated RNAs (selected by oligo-dT affinity) revealed that the majority of the *ASC1/snR24* hmsnoRNAs generated by anchoring away Slu7p were excluded from the oligo-dT selected population (Figure 2E). By contrast, the spliced and unspliced species were found in the oligodT-selected fraction. As expected, cleaved 5′-exon species and the *scR1* ncRNAs were also excluded from the poly(A)-selected RNAs (Figure 2E). We conclude that hmsnoRNAs are not polyadenylated at their 3′-end, which is consistent with their discrete band pattern on northern blots.

The previous mapping of hmsnoRNA by differential hybridization probing and 3′-RACE suggested that the 3′-ends of hmsnoRNA are generated by exonucleolytic trimming, which, for yeast snoRNAs is typically performed by the nuclear exosome [25]. To test the hypothesis that hmsnoRNA acquire their 3′-end through exosome-mediated processing, we used an anchor away strain where the nuclear exosome component Rrp6p is FRB-tagged. Anchoring away Rrp6p provides a more effective method of inactivating the nuclear exosome than deleting the gene encoding Rrp6p [26], possibly because exporting Rrp6p to the cytoplasm may also result in the nuclear depletion of other nuclear exosome components. We then generated a strain in which Rrp6p and Prp18p or Slu7p could be co-anchored away simultaneously. Nuclear depletion of Rrp6p resulted in an increased accumulation of both the unspliced and spliced forms of *NOG2* (Figure 3A). This observation is consistent with previous studies that showed that the nuclear exosome actively degrades unspliced precursors and may limit the production of mature species (Bousquet-Antonelli et al., 2000;Gudipati et al., 2012; Sayani and Chanfreau, 2012). Hybridization with a probe complementary to snR191 detected the accumulation of shortly extended forms of snR191 in the Rrp6p-AA strain (Supplemental Figure 2), consistent with the known role of the exosome in trimming intronic snoRNA mature 3′-ends [25].

As shown previously, anchoring away Slu7p (Figure 3A and Supplemental Figure 2) or Prp18p (Figure 3A), resulted in the accumulation of *NOG2-snR191* hmsnoRNAs. Strikingly, when Rrp6p was anchored away simultaneously with Prp18p or Slu7p, the accumulation of the hmsnoRNA decreased compared to what was observed when anchoring away these splicing factors alone (Figure 3A; see also Supplemental Figure 2 for Slu7p). We observed a concomitant increase in the level of unspliced precursors (Figure 3A, Supplemental Figure 2). This result suggested a precursor-to-product relationship between unspliced pre-mRNAs and hmsnoRNAs, and that hmsnoRNAs are generated by exonucleolytic trimming of unspliced precursors by the nuclear exosome.

Figure 3. HmsnoRNAs acquire their 3′-ends by trimming by the nuclear exosome but are mostly unaffected by cytoplasmic quality control pathways.

A. Northern blot analysis of *NOG2/snR191* in strains expressing FRB-tagged, anchor-away versions of Rrp6p, Prp18p, Slu7p, or double anchor away versions. Strains in the name of the gene italicized indicate that the corresponding protein was FRB-tagged (eg *rrp6* = *rrp6-FRB*). The membrane was hybridized with a probe complementary to the exon1 of *NOG2* . GAPDH was used as a loading control. Legends as in Figure 1.

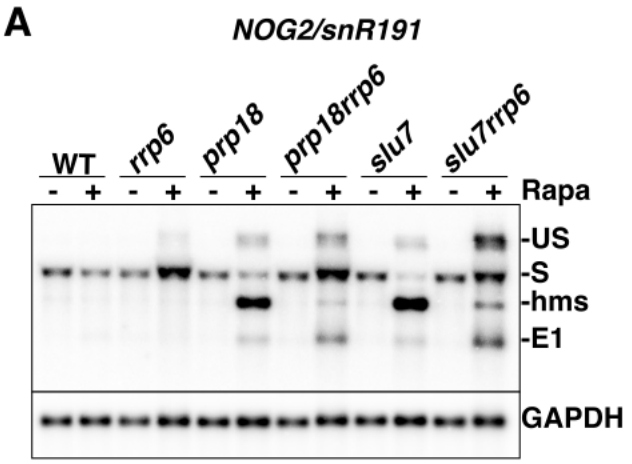

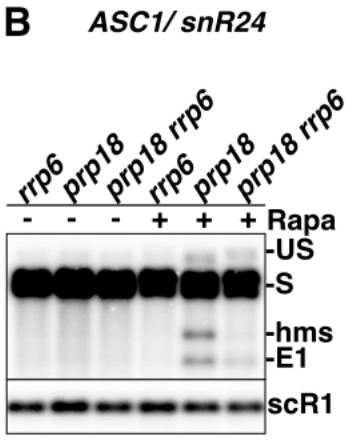

B. Northern blot analysis of *ASC1/snR191* in strains expressing FRB-tagged, anchor-away versions of Rrp6p, Prp18p, or both Prp18p and Rrp6p. The probe used was complementary to the exon1 of *ASC1*. Scr1 was used as a loading control. Labeling of the species as in (A).

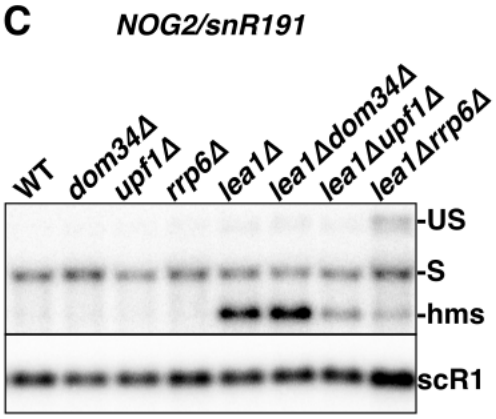

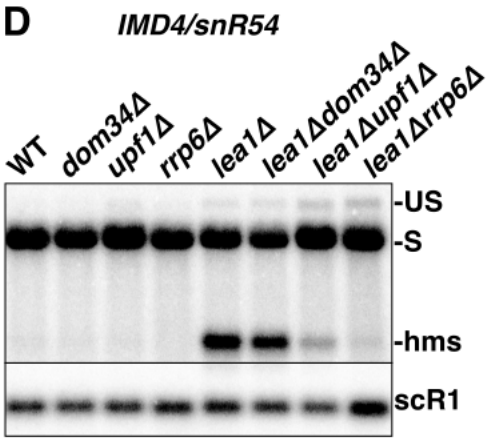

C. Northern blot analysis of *NOG2/snR191* in strains carrying viable deletions of the genes encoding the splicing factor Lea1p, and/or the RNA degradation or processing factors Dom34p, Upf1p or Rrp6p. The probe used is complementary to the exon1 of NOG2. scR1 was used as a loading control. Labeling of the species as in (A).

D. Analysis of IMD4/snR54 as described for NOG2/snR191 in panel C.

To further demonstrate that hmsnoRNAs are processed to or near the 3′-ends of the mature snoRNAs by the exosome, we used strains where the gene encoding the non-essential U2 snRNP component Lea1p is deleted, along with a deletion of the gene encoding Rrp6p. Consistent with the results obtained above, the *rrp6*Δ knockout resulted in a reduction in the accumulation of *NOG2-snR191* hmsnoRNA species when coupled to the *lea1*Δ mutation, accompanied by an accumulation of unspliced precursors (Figure 3C). Overall, these results combined with the 3′-RACE analyses described above show that hmsnoRNA are processed by the nuclear exosome to generate 3′-ends identical to those of the corresponding mature snoRNAs.

HmsnoRNAs are not targeted by translation-dependent quality control pathways.

Because hmsnoRNAs contain 5'-UTR and exon1 sequences, they exhibit mRNA-like features at their 5′-end which suggest that they might be translated. However, translation would stop shortly after the end of the 5′-exon sequence because of the occurrence of premature stop codons in the intronic sequences, which would trigger nonsense-mediated decay (NMD; He et al., 1993; Sayani et al., 2008). Alternatively, the presence of secondary structures in the snoRNAs or the binding by snoRNP proteins (see below) may block ribosome progression and trigger No-Go Decay (NGD; Doma and Parker, 2006). To investigate a potential targeting of hmsnoRNAs by these two RNA surveillance pathways, we knocked out the genes encoding the NMD factor Upf1p or the NGD factor Dom34p in the *lea1*Δ mutant and analyzed the *NOG2-snR191* and *IMD4-snR54* species by northern blot (Figure 3C, 3D). Eliminating Upf1p or Dom34p did not increase the levels of hmsnoRNAs in the *lea1*Δ mutant (Figures 3C and 3D). Instead, the *upf1*Δ knockout resulted in a decrease of the level of hmsoRNAs, while eliminating Dom34p showed no effect. As opposed to what was observed in the *lea1*Δ*rrp6*Δ mutant, the decreased accumulation of the *NOG2-snR191* hmsnoRNA detected in the *lea1*Δ*upf1*Δ mutant did not correlate with an increased accumulation of the unspliced precursors for snR191(Figure 3C), suggesting that Upf1p is not involved in the conversion of unspliced precursors into hmsnoRNAs. We detected some unspliced precursor accumulation for *IMD4* in the *lea1*Δ*upf1*Δ mutant (Figure 3D), but this was also detected in the *upf1*Δ

mutant. While we do not fully understand the molecular basis for the decreased accumulation of hmsnoRNAs in the *lea1*Δ*upf1*Δ mutant, experiments described below using splicing signals mutants suggest that this might be the result of indirect effects. Overall, we conclude from these experiments that hmsnoRNAs are not targeted by translation-mediated RNA quality control pathways.

HmsnoRNAs can be generated by a 5′ splice site mutation and are degraded by the major cytoplasmic decay pathway involving Xrn1p.

The previous results showed that inactivation of splicing factors resulted in the accumulation of hybrid mRNA-snoRNA species. However, we could not rule out that anchoring away splicing factors or deleting genes encoding non-essential splicing factors may result in indirect effects that may hamper the interpretation of our results. To alleviate these concerns, we used a plasmid-based system to introduce splice site mutations that would inhibit splicing and circumvent any general splicing defects. We generated a construct expressing the *NOG2-snR191* gene from a centromeric plasmid, which expressed NOG2 at levels that exceeded the RNAs expressed from the endogenous *NOG2* gene (Suppl.Figure 3). We did not detect any hmsnoRNA or any other aberrant species from the plasmid-borne wild-type version of *NOG2* showing that this version is fully and accurately processed (Suppl.Figure 3). We then generated two mutants designed to inactivate splicing of the plasmid borne *NOG2* transcripts: M1 is a mutation of the 5′-splice site (SS), and M2 is a double mutation that combines M1 with a branchpoint (BP) mutation (Figure 4A). Since the plasmid-borne versions are expressed at higher levels than the endogenous *NOG2* transcripts, and because *NOG2* is an essential gene, we used these plasmids in strains that also expressed the endogenous *NOG2* gene, which facilitated the genetic analysis. Transcripts expressed from the M1 and M2 plasmids accumulated in wild-type strains mostly as hmsnoRNAs, and to a lesser extent unspliced transcripts (Figure 4B). The temperature used to grow strains had some influence on the level of accumulation of hmsnoRNAs derived from these mutants, as hmsnoRNAs were more abundant when cells were grown at 20°C compared to 30°C (Suppl. Figure 4).

Figure 4. HmsnoRNAs generated by splice site mutations are degraded by Xrn1p and share some of the features of mature snoRNPs.

A. Mutations introduced in the plasmid expressing NOG2-snR191. 5′SS = 5′ splice site; BP = branchpoint.

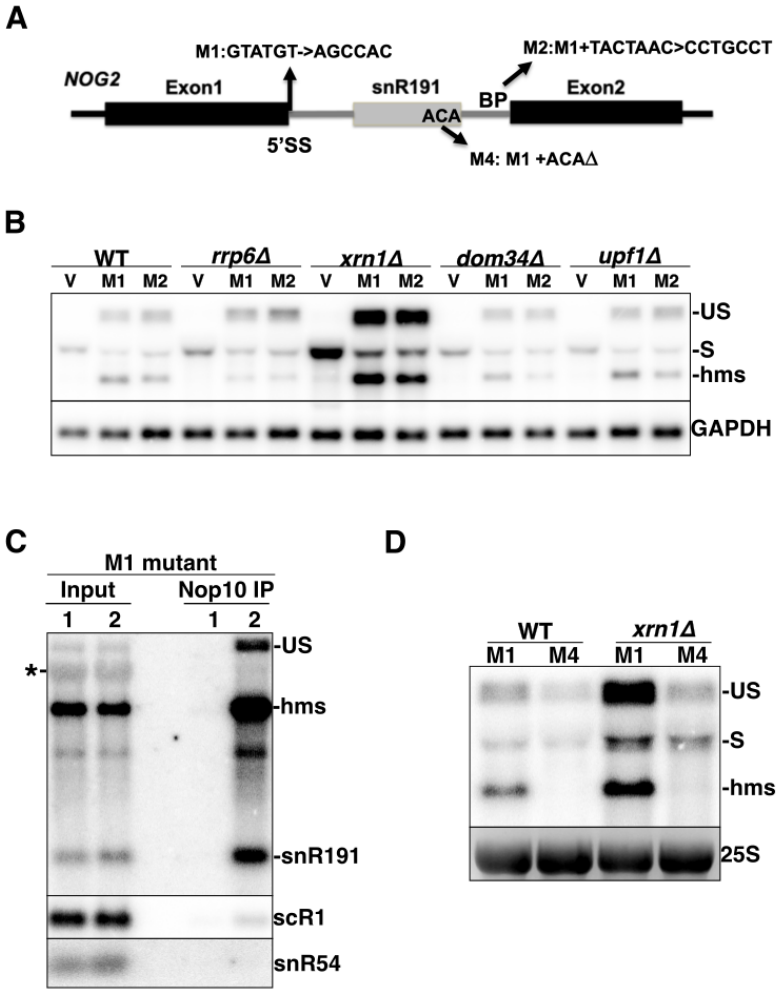

B. NOG2-snR191 hmsnoRNAs generated by splicing signal mutations are degraded by Xrn1p but unaffected by cytoplasmic quality control pathways. Wild-type (WT) or the indicated deletion mutants were transformed with the pUG35 vector (V) or the pUG35 plasmids expressing mutants M1 or M2 and RNAs extracted from these stains were analyzed by northern blot using a probe hybridizing to the exon1 of NOG2. GAPDH was used as a loading control. RNA species labeling as in Figure 1A.

C. NOG2-snR191 hmsnoRNAs generated by the M1 5′SS mutation are bound by the H/ACA snoRNP Nop10p. Shown are northern blots of RNAs extracted from cell extracts (Input) prepared from untagged wild-strain (Lane1) or ZZ-tagged Nop10 strain (Lane2) and of RNAs extracted after incubation of whole cell extracts from the same strains with IgG beads and washing (see methods). Membranes corresponding to independent purification experiments were hybridized to a probe complementary to the exon1 of NOG2 and to snR191 (top panel) or to probes hybridizing to scR1 or snR54 (bottom panels). The asterisk sign near the input lane indicates cross-hybridization of the probe to a ribosomal RNA.

D. Deletion of the ACA box of plasmid-borne *NOG2-snR191*destabilizes hmsnoRNAs generated by splicing signal mutations. Shown is a northern blot analysis using a probe hybridizing to the exon1 of *NOG2* of RNAs extracted from wild-type (WT), or *xrn1* deletion mutants transformed with plasmids expressing the M1 or M4 constructs (Figure 4A).

In the *rrp6*Δ mutant the levels of the hmsnoRNA expressed from the M1 or M2 plasmids decreased with an accumulation of unspliced precursors, consistent with our previous conclusion that the nuclear exosome processes the 3′-end of hmsnoRNAs. The *dom34*Δ and *upf1*Δmutations had no major effect on the accumulation of hmsnoRNAs, in contrast to the result described above which showed a decreased accumulation of hmsnoRNAs in the *lea1*Δ*upf1*Δ mutant (Figure 3D). Since inactivating Upf1p does not impact the level of hmsnoRNAs generated by splicing signal mutations, we interpret the decreased accumulation of hmsnoRNA previously described in the *lea1*Δ*upf1*Δ mutant as the result of indirect effects. This interpretation is supported by previous work showing that mutations that inactivate splicing and NMD result in synthetic growth defects[33], which may indirectly impair processes required for the accumulation of hmsnoRNAs.

In contrast to all other RNA degradation mutants analyzed previously, a large increase of all *NOG2* RNA species was detected in the *xrn1*Δ mutant deficient for the major cytoplasmic 5′-3′ exonuclease(Geisler and Coller, 2012) (Figure 4B). While the increased accumulation of the spliced and unspliced species was expected, the increase in abundance of the hmsnoRNA strongly suggests that these species are degraded in the cytoplasm by the general mRNA decay pathway, which relies primarily on Xrn1p. As hmsnoRNAs contain the 5′-ends and exon1 sequences of the *NOG2* gene, they may contain a ^{7}meG-cap similar to that of mRNAs which would subject them to the general decay pathway for cytoplasmic mRNAs (Mugridge et al., 2018). In order to show that hmsnoRNAs are degraded by the general cytoplasmic decay pathway which requires decapping, we analyzed hmsnoRNA accumulation resulting from the M1 mutation in a strain lacking the decapping enzyme Dcp2p (Suppl. Figure 5). As observed previously for the *xrn1*Δ mutant, inactivation of Dcp2p resulted in an increased accumulation of the hmsnoRNAs (Supplemental Figure 5). This result is consistent with the idea that hmsnoRNAs are degraded by the major cytoplasmic decay pathway, which involves Dcp1/2-mediated decapping and 5′-3′ decay by Xrn1p.

HmsnoRNAs share some of the hallmarks of mature snoRNAs

The plasmid expressing *NOG2* with a mutated 5′-SS provided us with a suitable system to investigate if hmsnoRNAs share some of the features of mature snoRNPs. We first asked if hmsnoRNAs are bound by a snoRNP protein found in mature snoRNP particles. We performed immunoprecipitation of RNAs in a strain expressing the *nog2*-M1 mutant and a ZZ-tagged version of Nop10, a core component of H/ACA snoRNPs [36]. A control strain was included which did not express the tagged version of Nop10p. Northern blot analysis of RNAs purified on IgG beads (which bind the ZZ-tagged Nop10p) showed that hmsnoRNAs co-purified with Nop10p, as did the mature forms of snR191 (Figure 4C, IP lane 2). By contrast, non H/ACA RNAs such as snR54 or scR1 ncRNA were not efficiently purified (Figure 4C and Suppl. Figure 6) and no RNAs were retained on IgG beads in the strain that did not express tagged Nop10p (IP lane 1), showing the specificity of this immunoprecipitation procedure. The ratio of signals for the RNAs found in the Nop10p immunoprecipitates compared to the input showed very similar values for the mature snR191 and the hmsnoRNAs (Suppl. Figure 6), suggesting that hmsnoRNAs are quantitatively bound by Nop10p. Interestingly, unspliced precursors were also immunoprecipitated by Nop10p (Figure 4C). This is consistent with prior work showing co-transcriptional assembly of H/ACA snoRNP proteins on an intron-encoded H/ACA snoRNA in *S.cerevisiae* [37].

If hmsnoRNA are bound by snoRNP proteins and stabilized by their binding, one would expect that a mutation of key snoRNA sequence elements that promote snoRNP assembly would result in a decrease of a steady-state levels of hmsnoRNAs, as described previously for mature H/ACA snoRNAs [1]. To test this hypothesis, we generated a variant of the M1 mutant in which the ACA box of the snR191 snoRNA is deleted (M4 mutant; Figure 4A), as mutation of the ACA box was previously shown to decrease H/ACA snoRNA accumulation [1]. This mutation resulted in the complete destabilization of the hmsnoRNA species, which were no longer detectable (Fig.4D). Deletion of of Xrn1p did not result in any detection of hmsnoRNAs for the M4 mutant, showing that the absence of hmsnoRNAs caused by deletion of the ACA box mutation is not due to an increased cytoplasmic turnover, but rather because of the lack of incorporation of the hmsnoRNA

into snoRNPs. We note that the overall levels of transcripts generated from the M4 mutant are lower than for the M1 mutant, suggesting that early binding of snoRNP proteins on the snR191 sequence contribute to early protection against degradation.

Discussion

In this work, we show that inactivation of splicing by impairing splicing factors or mutating splicing signals leads to the production of chimeric mRNA-snoRNA species containing the first exon, part of the intron and the intron-encoded snoRNA sequences for both box C/D or H/ACA snoRNAs. HmsnoRNA have extended 5′-ends containing mRNAs sequences that include 5′-UTR and exon1 and their 3′-ends match those of mature snoRNAs. The data presented above suggest a general pathway for the production and degradation of hmsnoRNAs (Figure 5). Splicing inactivation results in accumulation of unspliced pre-mRNAs, which are bound by at least a subpopulation of snoRNP proteins (eg Nop10p for the *NOG2-snR191* hmsnoRNA) and then trimmed to or near the mature 3′-end of the snoRNA sequence by the nuclear exosome (Figure 5). Early binding of snoRNP proteins is consistent with numerous studies that have shown co-transcriptional assembly of snoRNP components(Yang et al., 2005; Ballarino et al., 2005;,Bragantini et al., 2021; Darzacq et al., 2006). This assembly can occur in a splicing-independent manner [41], which explains why Nop10p can bind to hmsnoRNAs produced when splicing is inactivated (Figure 4) and why deletion of the ACA box of a *NOG2-snR191* gene containing a 5′-splice site mutant significantly destabilizes the RNAs generated from this construct. After nuclear 3′-end processing by the exosome, hmsnoRNAs are exported to the cytoplasm where they are degraded by the general 5′-3′ decay pathway that involves Dcp2p and Xrn1p (Figure 5).

Figure 5. Model of biogenesis of intron-encoded snoRNAs and impact of splicing inhibition on intron-encoded snoRNAs processing and degradation.

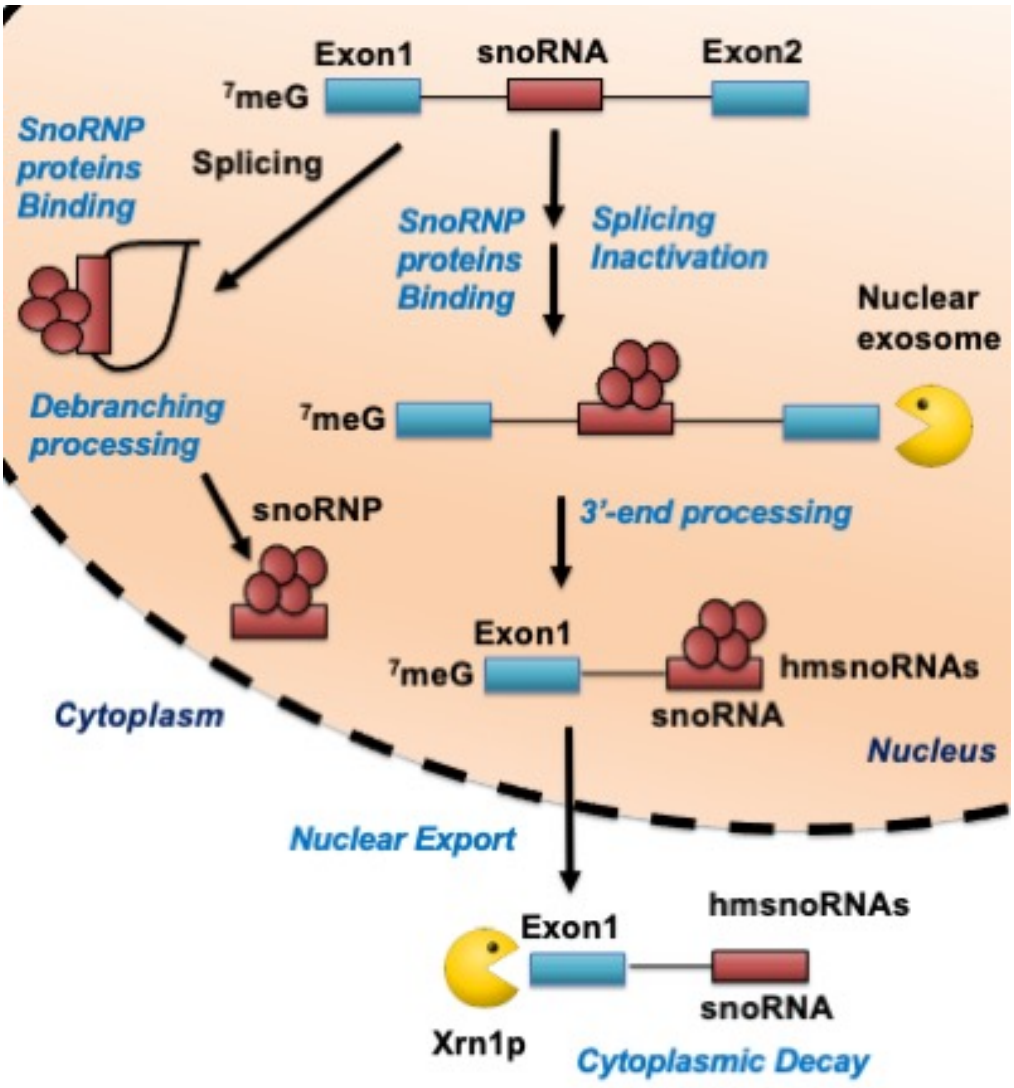

We found that inactivation of splicing factors involved at different steps of the spliceosome cycle results in the accumulation of hmsnoRNAs. This observation might be counterintuitive for 2nd catalytic step splicing factors such as Slu7p or Prp18p, as anchoring away these factors is expected to produce mostly lariat intermediates and cleaved 5′exons, but not unspliced precursors which are converted into hmsnoRNAs by

3′-5′ exonucleolytic activity of the nuclear exosome. However, a recent study from the Beggs lab offers an explanation to this conundrum, as inactivation of late splicing factors can result in unspliced precursors accumulation *in vivo* [42], possibly because of recycling defects. Our work sheds light onto previous results that described the accumulation of RNAs similar to hmsnoRNAs upon mutation of the branchpoint sequence of the host intron of snR18 (previously called U18)[43]. The result reported in this previous study is reminiscent of the effect detected when mutating the 5′-SS and the branchpoint of *NOG2*. In the previous study, the 5′-extended snR18 species were interpreted as intermediates in the processing pathway[43]. However, there was no evidence provided that these species could be converted into functional mature products, and based on our observations, it is more likely that they correspond to dead-end products similar to the ones that we characterized, and which are defective byproducts of splicing inactivation.

The accumulation of RNAs similar to hmsnoRNAs has also been reported when the pre-tRNA processing enzyme RNase P is inactivated by a thermosensitive (ts) mutation [17]. These species were considered intermediates in the pathway, and their accumulation was interpreted as evidence for a direct involvement of RNase P in the processing pathway of intron-encoded snoRNAs. However, RNase P-mediated cleavage intermediates could not be detected *in vivo* in this study [17]; furthermore, lariat introns containing snoRNAs accumulate at very high levels in a debranching enzyme mutant[12], which argues against a major cleavage pathway of intronic sequences by RNase P. We propose instead that the accumulation of hmsnoRNAs-like RNAs in the RNase P ts mutant is in fact due to an indirect inhibition of splicing, as work published later by the same group showed that this mutation results in the accumulation of unspliced pre-mRNA precursors *in vivo* [44] which might be converted into hmsnoRNAs.

Splicing activity has been shown to be inhibited during stress or non-standard growth conditions[45] which suggests that hmsnoRNAs could be naturally produced in such conditions without experimental interference with the splicing process. To assess whether hmsnoRNAs might be produced in growth conditions that reduce splicing efficiency, we

analyzed *NOG2* expression in stationary phase, heat shock conditions or treatment with rapamycin (in a wild-type strain that contains a functional TOR pathway, unlike the anchor away strains described above). None of these conditions resulted in the accumulation of hmsnoRNAs (Suppl.Fig.7). However, the same conditions are also known to generally reduce ribosome biogenesis and snoRNP assembly. Therefore, the absence of detection of these species in these conditions is difficult to interpret, as it might be due to conditions that globally repress ribosome biogenesis and prevent assembly of snoRNP proteins on the hmsnoRNA species.

The results presented here provide a general framework that underscores the importance of the splicing process for the biogenesis of snoRNAs. In the absence of splicing, not only are intron-encoded snoRNAs not processed properly, but the RNAs species that are improperly generated are subject to a degradation pathway similar to that which targets mRNAs in the cytoplasm (Figure 6). A parallel model was proposed to underscore the importance of 5′-end processing for independently transcribed snoRNAs in *S.cerevisiae* [18]. In the absence of co-transcriptional cleavage of snoRNA precursors by the endonuclease Rnt1p, unprocessed snoRNAs accumulate in the cytoplasm and are not functional[18]. Overall, the results described here combined to those reported by Kufel, Proudfoot and colleagues converge to establish a unified model for the importance of RNA processing for the fate of snoRNAs. Regardless of the precise mode of expression and of the nature of the transcription units that produce snoRNAs, RNA processing of snoRNA precursors serves two major purposes: these reactions not only remove flanking sequences, but also dictate the proper fate of snoRNP particles and their mode of degradation. In the case of intron-encoded snoRNAs, the work described here establishes an additional functional role for splicing reactions, beyond simply removing intervening sequences of mRNAs. Finally, these data may shed some light onto the molecular effects of mutations of splicing factors, which can result in a variety of human diseases. While the impact of these mutations on mRNA splicing and alternative splicing patterns has been investigated, their effect on the production of intron-encoded snoRNAs has not been well characterized. It is possible that some of the deleterious effects of these

mutations that are causal to disease may be linked to the defective processing of intron-encoded snoRNAs and the production of hmsnoRNA-like species, which may be detrimental to RNA metabolism.

Methods

Yeast strain construction and manipulation, RNA extraction and northern blot analysis using riboprobes was performed as described in Wang et al [46]. The list of strains and oligonucleotides used is provided in supplementary information. Wild-type and knockout yeast strains are from the BY4742 genetic background[47] and knockout strains were obtained from the systematic knockout collection[48]. Strains used for the anchor away experiments are from the HHY168 genetic background[20]. For the expression of *NOG2* mutants, the wild-type *NOG2* gene was cloned in pUG35[49] and expressed under the control of its own promoter to create pCL1. The M1, M2 and M4 mutants were created by site-directed mutagenesis from pCL1. For immunoprecipitation of ZZ-tagged Nop10p, we used strains transformed with the pFH35 plasmid that expresses ZZ-tagged Nop10p[36]. RNA immunoprecipitation was performed as following: yeast cells corresponding to 400 OD600 units of culture were harvested in exponential phase, washed and resuspended in lysis buffer (20mM Tris-HCl pH=8, 300mM K-Acetate, 5mM $MgCl_2$, 1mM Dithiothreitol, 0.2% Triton X-100, protease inhibitors cocktail tablet (Roche)). Cells were lysed by vortexing in the presence of glass beads (425-600 µm) for 5 minutes. Whole cell lysates were collected after centrifugation at 15,000 rpm for 20 minutes. About 1000µL of lysate and 50µL of pre-washed mouse IgG conjugated magnetic beads (Cell Signaling) were incubated for one hour on a shaker at 4°C. After purification of the beads on a magnetic rack, beads were washed five times with 1000µL of lysis buffer and RNA extraction after the final wash were performed using phenol: chloroform: iso-amyl alcohol solution (VWR).

Acknowledgements: We thank Dr Anthony Henras for sharing the Nop10-ZZ tagged expression plasmid and for helpful suggestions, and Dr Jeffery Coller for providing the dcp2 mutant strain, respectively. This work was supported by the National Institute of General Medical Sciences (grant R35 GM130370 to G.F.C).

References

1. Balakin, A. G., Smith, L. & Fournier, M. J. The RNA world of the nucleolus: two major families of small RNAs defined by different box elements with related functions. *Cell* **86**, 823-834. (1996).
2. J, K. & P, G. Small Nucleolar RNAs Tell a Different Tale. *Trends in genetics : TIG* **35**, 104–117 (2019).
3. Kiss, T. Small nucleolar RNA-guided post-transcriptional modification of cellular RNAs. *EMBO J.* **20**, 3617-3622. (2001).
4. Liang, J. *et al.* Small Nucleolar RNAs: Insight Into Their Function in Cancer. *Frontiers in Oncology* **9**, 587 (2019).
5. Faucher-Giguère, L. *et al.* High-grade ovarian cancer associated H/ACA snoRNAs promote cancer cell proliferation and survival. *NAR cancer* **4**, (2022).
6. Cavaillé J. Box C/D small nucleolar RNA genes and the Prader-Willi syndrome: a complex interplay. *Wiley interdisciplinary reviews. RNA* **8**, (2017).
7. Schaffer, J. E. Death by lipids: The role of small nucleolar RNAs in metabolic stress. *Journal of Biological Chemistry* **295**, 8628–8635 (2020).
8. Brown JW, Marshall DF & Echeverria M. Intronic noncoding RNAs and splicing. *Trends in plant science* **13**, 335–342 (2008).
9. Lykke-Andersen, S. *et al.* Human nonsense-mediated RNA decay initiates widely by endonucleolysis and targets snoRNA host genes. *Genes and Development* **28**, 2498–2517 (2014).
10. Fafard-Couture, É., Bergeron, D., Couture, S., Abou-Elela, S. & Scott, M. S. Annotation of snoRNA abundance across human tissues reveals complex snoRNA-host gene relationships. *Genome Biology* **22**, (2021).
11. Kiss, T. & Filipowicz, W. Exonucleolytic processing of small nucleolar RNAs from pre-mRNA introns. *Genes Dev* **9**, 1411–1424 (1995).
12. Ooi, S. L., Samarsky, D. A., Fournier, M. J. & Boeke, J. D. Intronic snoRNA biosynthesis in Saccharomyces cerevisiae depends on the lariat-debranching enzyme: intron length effects and activity of a precursor snoRNA. *RNA* **4**, 1096-1110. (1998).
13. Ghazal, G., Ge, D., Gervais-Bird, J., Gagnon, J. & Abou Elela, S. Genome-Wide Prediction and Analysis of Yeast RNase III-Dependent snoRNA Processing Signals. *Mol Cell Biol* **25**, 2981–2994 (2005).
14. Hirose, T., Shu, M. D. & Steitz, J. A. Splicing-dependent and -independent modes of assembly for intron-encoded box C/D snoRNPs in mammalian cells. *Mol Cell* **12**, 113–123 (2003).
15. Caffarelli, E., Arese, M., Santoro, B., Fragapane, P. & Bozzoni, I. In vitro study of processing of the intron-encoded U16 small nucleolar RNA in Xenopus laevis. *Mol Cell Biol* **14**, 2966–2974 (1994).
16. Cecconi, F., Mariottini, P. & Amaldi, F. The Xenopus intron-encoded U17 snoRNA is produced by exonucleolytic processing of its precursor in oocytes. *Nucleic acids research* **23**, 4670–4676 (1995).
17. Coughlin, D. J., Pleiss, J. A., Walker, S. C., Whitworth, G. B. & Engelke, D. R. Genome-wide search for yeast RNase P substrates reveals role in maturation of intron-encoded box C/D

small nucleolar RNAs. *Proceedings of the National Academy of Sciences* **105**, 12218–12223 (2008).

18. Grzechnik, P. *et al.* Nuclear fate of yeast snoRNA is determined by co-transcriptional Rnt1 cleavage. *Nature Communications 2018 9:1* **9**, 1–14 (2018).
19. Scruggs, B. S., Michel, C. I., Ory, D. S. & Schaffer, J. E. SmD3 Regulates Intronic Noncoding RNA Biogenesis. *Molecular and Cellular Biology* **32**, 4092–4103 (2012).
20. Haruki, H., Nishikawa, J. & Laemmli, U. K. The Anchor-Away Technique: Rapid, Conditional Establishment of Yeast Mutant Phenotypes. *Molecular Cell* **31**, 925–932 (2008).
21. Wahl, M. C., Will, C. L. & Luhrmann, R. The spliceosome: design principles of a dynamic RNP machine. *Cell* **136**, 701–718 (2009).
22. Badis, G., Fromont-Racine, M. & Jacquier, A. A snoRNA that guides the two most conserved pseudouridine modifications within rRNA confers a growth advantage in yeast. *RNA* **9**, 771–779 (2003).
23. Caspary, F. & Séraphin, B. The yeast U2A'/U2B" complex is required for pre-spliceosome formation. *The EMBO Journal* **17**, 6348–6358 (1998).
24. Villa, T. & Guthrie, C. The Isy1p component of the NineTeen complex interacts with the ATPase Prp16p to regulate the fidelity of pre-mRNA splicing. *Genes Dev* **19**, 1894–1904 (2005).
25. Allmang, C. *et al.* Functions of the exosome in rRNA, snoRNA and snRNA synthesis. *EMBO J* **18**, 5399–5410 (1999).
26. Roy, K., Gabunilas, J., Gillespie, A., Ngo, D. & Chanfreau, G. F. Common genomic elements promote transcriptional and DNA replication roadblocks. *Genome Research* **26**, 1363–1375 (2016).
27. Bousquet-Antonelli, C., Presutti, C. & Tollervey, D. Identification of a regulated pathway for nuclear pre-mRNA turnover. *Cell* **102**, 765–775 (2000).
28. Sayani, S. & Chanfreau, G. F. Sequential RNA degradation pathways provide a fail-safe mechanism to limit the accumulation of unspliced transcripts in Saccharomyces cerevisiae. *RNA (New York, N.Y.)* **18**, 1563–72 (2012).
29. Gudipati, R. K. *et al.* Extensive degradation of RNA precursors by the exosome in wild-type cells. *Mol Cell* **48**, 409–421 (2012).
30. He, F., Peltz, S. W., Donahue, J. L., Rosbash, M. & Jacobson, A. Stabilization and ribosome association of unspliced pre-mRNAs in a yeast upf1- mutant. *Proc Natl Acad Sci U S A* **90**, 7034–7038 (1993).
31. Sayani, S., Janis, M., Lee, C. Y., Toesca, I. & Chanfreau, G. F. Widespread Impact of Nonsense-Mediated mRNA Decay on the Yeast Intronome. *Molecular Cell* **31**, 360–370 (2008).
32. Doma, M. K. & Parker, R. Endonucleolytic cleavage of eukaryotic mRNAs with stalls in translation elongation. *Nature* **440**, 561–564 (2006).
33. Kawashima, T., Pellegrini, M. & Chanfreau, G. F. Nonsense-mediated mRNA decay mutes the splicing defects of spliceosome component mutations. *RNA* **15**, 2236–47 (2009).
34. Geisler S & Coller J. XRN1: A Major 5' to 3' Exoribonuclease in Eukaryotic Cells. *The Enzymes* **31**, 97–114 (2012).

35. Mugridge JS, Coller J & Gross JD. Structural and molecular mechanisms for the control of eukaryotic 5'-3' mRNA decay. *Nature structural & molecular biology* **25**, 1077–1085 (2018).
36. Dez, C. *et al.* Stable expression in yeast of the mature form of human telomerase RNA depends on its association with the box H/ACA small nucleolar RNP proteins Cbf5p, Nhp2p and Nop10p. *Nucleic Acids Res* **29**, 598–603 (2001).
37. Yang, P. K. *et al.* Cotranscriptional recruitment of the pseudouridylsynthetase Cbf5p and of the RNA binding protein Naf1p during H/ACA snoRNP assembly. *Mol Cell Biol* **25**, 3295–3304 (2005).
38. Ballarino, M., Morlando, M., Pagano, F., Fatica, A. & Bozzoni, I. The cotranscriptional assembly of snoRNPs controls the biosynthesis of H/ACA snoRNAs in Saccharomyces cerevisiae. *Mol Cell Biol* **25**, 5396–5403 (2005).
39. Darzacq, X. *et al.* Stepwise RNP assembly at the site of H/ACA RNA transcription in human cells. *J Cell Biol* **173**, 207–218 (2006).
40. Bragantini, B. *et al.* The box C/D snoRNP assembly factor Bcd1 interacts with the histone chaperone Rtt106 and controls its transcription dependent activity. *Nature Communications 2021 12:1* **12**, 1–17 (2021).
41. Richard, P., Kiss, A. M., Darzacq, X. & Kiss, T. Cotranscriptional recognition of human intronic box H/ACA snoRNAs occurs in a splicing-independent manner. *Mol Cell Biol* **26**, 2540–2549 (2006).
42. Mendoza-Ochoa GI, Barrass JD, Maudlin IE & Beggs JD. Blocking late stages of splicing quickly limits pre-spliceosome assembly in vivo. *RNA biology* **16**, 1775–1784 (2019).
43. Villa, T., Ceradini, F. & Bozzoni, I. Identification of a novel element required for processing of intron-encoded box C/D small nucleolar RNAs in Saccharomyces cerevisiae. *Mol Cell Biol* **20**, 1311–1320 (2000).
44. Marvin, M. C. *et al.* Accumulation of noncoding RNA due to an RNase P defect in Saccharomyces cerevisiae. *RNA* **17**, 1441–1450 (2011).
45. Pleiss, J. A., Whitworth, G. B., Bergkessel, M. & Guthrie, C. Rapid, transcript-specific changes in splicing in response to environmental stress. *Mol Cell* **27**, 928–937 (2007).
46. Wang, C. *et al.* Rrp6 Moonlights in an RNA Exosome-Independent Manner to Promote Cell Survival and Gene Expression during Stress. *Cell Reports* **31**, (2020).
47. Brachmann, C. B. *et al.* Designer deletion strains derived from Saccharomyces cerevisiae S288C: a useful set of strains and plasmids for PCR-mediated gene disruption and other applications. *Yeast (Chichester, England)* **14**, 115–132 (1998).
48. Winzeler, E. A. *et al.* Functional characterization of the S. cerevisiae genome by gene deletion and parallel analysis. *Science (New York, N.Y.)* **285**, 901–906 (1999).
49. Niedenthal, R. K., Riles, L., Johnston, M. & Hegemann, J. H. Green fluorescent protein as a marker for gene expression and subcellular localization in budding yeast. *Yeast* **12**, 773–786 (1996).